Title
Biosynthesis of Isonitrile- and Alkyne-Containing Natural Products

Journal
Annual Review of Chemical and Biomolecular Engineering, 13(1)

ISSN
1947-5438

Authors
Del Rio Flores, Antonio
Barber, Colin C
Narayanamoorthy, Maanasa
et al.

Publication Date
2022-06-10

DOI
10.1146/annurev-chembioeng-092120-025140

Peer reviewed

HHS Public Access

Author manuscript

Annu Rev Chem Biomol Eng. Author manuscript; available in PMC 2023 January 04.

Published in final edited form as:

Annu Rev Chem Biomol Eng. 2022 June 10; 13: 1–24. doi:10.1146/annurev-chembioeng-092120-025140.

Biosynthesis of Isonitrile- and Alkyne-Containing Natural Products

Antonio Del Rio Flores[1], **Colin C. Barber**[2], **Maanasa Narayanamoorthy**[3], **Di Gu**[3], **Yuanbo Shen**[3], **Wenjun Zhang**[1,4]

[1]Department of Chemical and Biomolecular Engineering, University of California, Berkeley, California, USA

[2]Department of Plant and Microbial Biology, University of California, Berkeley, California, USA

[3]Department of Chemistry, University of California, Berkeley, California, USA

[4]Chan Zuckerberg Biohub, San Francisco, California, USA

Abstract

Natural products are a diverse class of biologically produced compounds that participate in fundamental biological processes such as cell signaling, nutrient acquisition, and interference competition. Unique triple-bond functionalities like isonitriles and alkynes often drive bioactivity and may serve as indicators of novel chemical logic and enzymatic machinery. Yet, the biosynthetic underpinnings of these groups remain only partially understood, constraining the opportunity to rationally engineer biomolecules with these functionalities for applications in pharmaceuticals, bioorthogonal chemistry, and other value-added chemical processes. Here, we focus our review on characterized biosynthetic pathways for isonitrile and alkyne functionalities, their bioorthogonal transformations, and prospects for engineering their biosynthetic machinery for biotechnological applications.

Keywords

natural products; enzymology; biosynthesis; bioorthogonal chemistry

1. INTRODUCTION

Natural products (NPs) are structurally diverse compounds leveraged for their pharmaceutical potential in treating human health conditions including cancer, autoimmune disorders, infections, and cardiovascular disease. These specialized metabolites are produced by microbes as a result of evolutionary pressure to mediate crucial biological and ecological functions, including signaling, interference competition, biofilm formation, virulence, and nutrient acquisition (1–5).

antonio_delrioflores@berkeley.edu .

DISCLOSURE STATEMENT

The authors are not aware of any affiliations, memberships, funding, or financial holdings that might be perceived as affecting the objectivity of this review.

Nature has endowed NPs with astonishing structural complexity and diversity, a key attribute motivating chemical engineers and chemists to couple biosynthetic and synthetic strategies to sustainably produce novel bioactive compounds. For example, despite the limited building blocks present in Nature compared to in synthetic chemistry, biosynthetic enzymes can generate and install unusual functional groups, like isonitriles and alkynes, on complicated small-molecule scaffolds with unmatched selectivity. Yet, even if a biosynthetic gene cluster (BGC) and the structure of its small-molecule product are known, rigorous understanding of the enzymology undergirding unusual functional group biosynthesis is often elusive, presenting a significant roadblock to engineering scaffolds harboring the target functional group (6). Thus, thoroughly understanding NP biosynthesis and unusual functional group biosynthesis specifically is vital for applying engineered biocatalysts to produce value-added compounds containing desired chemical scaffolds and may facilitate functional group-guided NP discovery.

We focus our review on two unusual functional groups, isonitriles and alkynes. These unique functionalities commonly behave as bioactive warheads of NPs and possess distinct physical and chemical properties of interest in chemical biology (7). We first discuss known biosynthetic routes to generate these functionalities. We further discuss isonitriles and alkynes as clickable, bioorthogonal functionalities of use in chemical biology applications. Last, we discuss prospects for and advances in engineering isonitrile and alkyne biosynthetic machinery in biotechnology. We direct the reader's attention to other recent reviews covering isonitrile and alkyne biosynthesis (8–13). We aim to update and further accentuate the wealth of literature associated with isonitrile and alkyne biosynthesis, mechanistic studies, bioorthogonal chemistry, and engineering of biocatalysts to afford these unique functionalities.

2. ISONITRILE BIOSYNTHESIS AND ENGINEERING

The isonitrile functional group decorates more than 200 NPs originating from marine and terrestrial organisms that drive virulence, detoxification, metal acquisition, and antimicrobial activity phenotypes (14–16). Isonitrile-bearing NPs have been isolated and characterized from diverse organisms such as fungi (17, 18), bacteria (14, 15, 19), cyanobacteria (20), plants (21), marine sponges (22, 23), and nudibranch mollusks (24). It was first proposed that the isonitrile moiety was incorporated into terpene molecules through inorganic cyanide incorporation in marine sponges (25, 26). Many isonitrile-bearing NPs have been isolated from marine sponges, beginning with the discovery of axisocyanide-1 reported in 1973 from *Axinella cannabina* (22, 23). Despite the precedent of these metabolites, their biosynthesis remains relatively unknown owing to competing hypotheses regarding the origin of the isonitrile group. The consensus is that isonitrile formation occurs nonenzymatically through inorganic cyanide incorporation into marine NPs (22, 23). Cyanides putatively originate from oxidative degradation of glycine in bacteria, where they can expeditiously diffuse to sponge tissues under physiological conditions as hydrogen cyanide (8). Multiple studies have fed labeled amino acid substrates (e.g., glycine, serine, tyrosine) as well as labeled acetate to sponge cultures, yet incorporation of the labeled atoms has not been detected in the isonitrile products (27, 28). However, feeding of sodium-^{14}C-cyanide to *Amphimedon* sponges resulted in ^{14}C incorporation into the final diisocyanoadociane product, and feeding

of doubly labeled $^{13}C,^{15}N$-cyanide to the sponge *Ciocalypta* sp. resulted in the retention of both labeled atoms in the final isonitrile-containing product (25, 28). These data from early studies suggest a mechanism for isonitrile biosynthesis in which the cyanide is of abiotic origin and is incorporated directly into the NP scaffold. Alternatively, it is possible that sponges themselves are incapable of producing isonitrile products altogether, and instead, their bacterial symbionts may produce them (26). Currently, there are two characterized biosynthetic routes for isonitrile biogenesis: first, through isonitrile synthases (represented by IsnA), and second, through nonheme iron(II) [Fe(II)]–dependent and α-ketoglutarate (α-KG)-dependent dioxygenases [Fe(II)/α-KG-dioxygenase] found in *Actinobacteria* (29, 30).

2.1. Isonitrile Biosynthesis by IsnA Family

The first biosynthetic pathway for isonitriles was discovered from an experiment analyzing the biosynthetic potential of uncultured soil bacteria by employing a high-throughput antibacterial phenotypic screen (31). Environmental DNA was isolated from New York soil by heating with detergent, chloroform extraction, isopropanol precipitation, and a final gel-purification step. The resulting environmental DNA was cloned into a cosmid library and expressed in *Escherichia coli*, and the library was screened for antibacterial activity using a growth inhibition assay against *Bacillus subtilis* in an agar overlay. Cosmid libraries are composed of cosmids, which are special types of plasmids containing a cos site that are commonly used to clone large genomic regions. Clones from the growth inhibition assay that produced a zone of inhibition were recovered and screened for antibacterial culture extracts (31–35). A bioassay-guided fractionation strategy was used to isolate the potent antibiotic *trans*-**1** containing an isonitrile-functionalized C-3-substituted indole with a *trans*-olefin (Figure 1a). The genes responsible for biosynthesis of *trans*-**1** were identified by dissecting the producing cosmid with transposons. Transposon insertions essentially inactivate a specific gene, meaning that the biosynthetic gene(s) for a compound can be deduced by identifying the transposon insertion(s) that abrogate its production. These two genes were identified as *isnA* and *isnB*, encoding an isonitrile synthase and a Fe(II)/α-KG-dioxygenase, respectively (29) (Figure 1a). The chemical structure of *trans*-**1** suggested that the nitrogen atom originated from the α-amino group of an indole-containing amino acid. To test this hypothesis, doubly labeled ^{15}N-L-tryptophan was fed to a tryptophan auxotroph and transaminase-deficient *E. coli* culture expressing *isnA*/*isnB* that resulted in incorporation of both ^{15}N labels, thus demonstrating that both nitrogen atoms from *trans*-**1** originate from L-tryptophan. The tryptophan auxotrophy and transaminase deficiency were used to ensure that only the ^{15}N-L-tryptophan variant (not unlabeled) was present in the culture and to make sure it was not lost during the feeding experiment, respectively. The biosynthesis of *trans*-**1** was investigated by overexpressing IsnA and IsnB as glutathione-S-transferase (GST) fusion proteins in cultures of *E. coli*. Both IsnA-GST and IsnB-GST were required for production of *trans*-**1** and feeding of compound **3** to a culture expressing IsnB-GST-produced **1** (Figure 1a). Promiscuous bacterial esterases present in *E. coli* were shown to slowly degrade compound **3** to **2** (Figure 1a). These studies demonstrate that IsnA catalyzes the formation of the isonitrile moiety on the α-amino group of L-tryptophan with an unknown carbon source and IsnB mediates the oxidative decarboxylation of **2** to yield *trans*-**1** (29) (Figure 1a). The origin of the carbon source was investigated with an inverse-

labeling experiment in which the metabolome was dissected by heterologously expressing *isnA*/*B* in *E. coli* knockout mutants missing genes at each major branch point of sugar metabolism. Cultures were fed ^{13}C glucose to generate a ^{13}C-labeled metabolic background, followed by feeding with ^{12}C glucose substrates to chemically complement the generated knockout mutants. To identify the branchpoint associated with isonitrile biosynthesis, *trans*-**1** lacking ^{13}C incorporation was identified, confirming that ribulose-5-phosphate (R-5-P) is the co-substrate and carbon source for the IsnA enzymatic reaction (Figure 1a). Feeding of C1- and C2-labeled ^{13}C-R-5-P to *E. coli* cultures expressing *isnA*/*isnB* further demonstrated that C2 of R-5-P is the carbon donor for the isonitrile group in *trans*-**1** (36) (Figure 1a). The isotope tracer experiment results have led to speculation of an imine intermediate formed to link the keto carbon (C2) from R-5-P and the α-amino group of L-tryptophan. This potential intermediate may be formed from a nucleophilic attack of the α-amine of L-tryptophan, followed by subsequent dehydration to yield the imine. The rest of the mechanism is thought to proceed via β-keto imine formation, resulting in loss of hydroxyacetone and final release of compound *trans*-**1** and formaldehyde (8, 37) (Figure 1b). The precise catalytic mechanism for IsnA synthases remains elusive. To date, PvcA is the only enzyme from the IsnA family with a solved 3D structure (38). Drake & Gulick (38) showed that PvcA has a modified Rossman fold with a central five-stranded β-sheet surrounded with α-helices on both sides. Additionally, PvcA has a smaller C-terminal domain containing a second β-sheet with a single helix. Owing to the crystallization conditions, a phosphate ion was bound to the putative active site of PvcA, suggesting that a sugar phosphate substrate is used as the carbon donor. Four key residues are proposed to play a role in the phosphate binding pocket: Arg251, Ser253, His255, and Lys263 (38). Catalytic insight into the mechanism will benefit from substrate-bound structures and identification of putative reaction intermediates. This section covers known isonitrile biosynthesis of NPs derived from L-tyrosine and L-tryptophan building blocks from the IsnA family.

2.1.1. Tyrosine-derived isonitrile biosynthesis.—

Xanthocillin, isolated in the 1950s from *Penicillium notatum*, was the first known isonitrile-containing NP (39). Despite the early discovery of xanthocillin, the biosynthetic genes associated with isonitrile formation were not identified until 2005, and its biosynthesis was not elucidated until 2018 (18, 29). Xanthocillin is a diisonitrile chalkophore produced by *Penicillium* spp. and the human pathogen *Aspergillus fumigatus*. Genome mining for IsnA homologs revealed the existence of the *xan* BGC encoding the putative isonitrile synthase XanB and the cytochrome P450 XanG. The pathway uses L-tyrosine as the α-amino nitrogen-donating substrate. XanB, a didomain enzyme, mediates the formation of the isonitrile moiety with the N-terminal isonitrile synthase domain, followed by subsequent decarboxylation and desaturation of the L-tyrosine scaffold by the C-terminal nonheme Fe(II) α-KG-dependent dioxygenase domain to yield **4** (18) (Figure 1c). In contrast to the previously established IsnA pathway, the xanthocillin biosynthetic pathway requires only one enzyme, XanB, to both establish the isonitrile functionality and olefinate the isonitrile intermediate. The cytochrome P450 XanG is coregulated with XanB and subsequently converts two units of **4** to xanthocillin. Upon dimerization by XanG, the methyl transferase XanE is proposed to act next in the biosynthetic pathway to yield the methylated derivative BU-4704. R-5-P has not been confirmed as the carbon donor source required for isonitrile

installation. The dimerization of two isonitrile-derived intermediates has also been observed in *Saccharomyces cerevisiae*. The isonitrile synthase Dit1 converts L-tyrosine to **5** in the same way as XanB (40). Unlike XanB, Dit1 does not olefinate this intermediate; instead, the isonitrile product is converted to N-formyl tyrosine, presumably through nonenzymatic hydrolysis (40). The cytochrome P450 Dit2 subsequently dimerizes N-formyl tyrosine to form N,N-bisformyltyrosine.

The isonitrile-containing dihydroxycumarin, paerucumarin, is produced by *Pseudomonas aeruginosa*, a human pathogen commonly associated with acute respiratory, chronic respiratory, and pulmonary infections (41). It was first characterized in 2008 after investigation of the role of the *pvc* gene cluster in *P. aeruginosa*, which was linked to biofilm development through the enhancement of the chaperone/usher (*cup*) gene cluster and the production of a fluorescent metabolite similar to pyoverdine chromophores (14, 41, 42). Investigation of the paerucumarin biosynthetic pathway revealed the enzymes PvcA and PvcB, an isonitrile synthase and a Fe(II)/α-KG-dioxygenase, respectively (14). PvcA generates **5** with L-tyrosine as the nitrogen donor. R-5-P has not been confirmed as the carbon source for isonitrile formation in paerucumarin biosynthesis (Figure 1c). Then **5** undergoes oxidative decarboxylation by PvcB to yield **4** (Figure 1c). PvcC and PvcD, related to the two-component flavin adenine dinucleotide-dependent monooxygenases HpaB and HpaC, further oxidize **4** to a catechol that undergoes an intermolecular cyclization with the carboxylate functionality to produce paerucumarin (37). Owing to the instability of the isonitrile moiety, paerucumarin has been known to decompose to an N-formyl adduct (14). Bioinformatic analysis revealed homologous biosynthetic pathways in the insect pathogen *Photorhabdus luminescens*, the plant pathogen *Erwinia carotovorum*, and the bacterial predator *Bdellovibrio bacteriovorus* and in human pathogens including *Burkholderia mallei*, *Vibrio cholera*, and *Legionella pneumophila* (14).

Rhabduscins are amidoglycosyl- and vinyl-isonitrile-functionalized L-tyrosine-derived metabolites identified in *Xenorhabdus* and *Photorhabdus* strains (7). These compounds are well-known for their role as insect phenoloxidase inhibitors, which have been linked to the inhibition of mushroom tyrosinases. Genome mining of homologous BGCs with IsnA and IsnB homologs revealed the presence of the gene clusters *XNC1_1221-XNC1_1223* in *X. nematophila* and *plu2816-plu2817* in *P. luminescens* (15). The IsnA homologs XnPvcA (*X. nematophila*) and PlPvcA (*P. luminescens*) install an isonitrile moiety from the α-amino nitrogen of L-tyrosine and a donor carbon atom from R-5-P to yield **5** (Figure 1c). The IsnB homologs XnPvcB and PlPvcB then olefinate **5** in *X. nematophila* and *P. luminescens*, respectively, producing **4** (Figure 1c). Rhabduscin BGCs in *X. nematophila* and *P. luminescens* contain not only the *isnA* and *isnB* homologs but also the glycosyltransferase genes *XNC1_1223* and *plu1760-plu1762* that presumably convert **4** into rhabduscin. The specific function of these glycosyltransferases in the rhabduscin biosynthetic pathway is not well understood, but they have been hypothesized to either transfer activated sugars to the vinyl isonitrile aglycone or have redundant enzymatic function (7). Remarkably, the rhabduscin biosynthetic pathway has been observed to spontaneously generate daughter metabolites known as rhabdoplanins, which were produced by *X. bovienii* through an Ugi-like multicomponent reaction that resembles the historical multicomponent Ugi reaction

commonly used in synthetic chemistry (43). Furthermore, **4** was proposed to be an intermediate for the isothianocyanate metabolite sinapigladioside in *Burkholderia* species (44). Although the enzymes(s) for sulfur incorporation were not identified, isotope labeling and bioinformatic analyses support the intermediacy of an isonitrile metabolite with one IsnA homolog (SpgA) and a fusion protein with a N-terminal IsnA domain and C-terminal IsnB domain (SpgD) encoded within the putative *spg* BGC (44).

2.1.2. Tryptophan-derived isonitrile biosynthesis.—

The isonitrile moiety is also a feature in terpenoid indole alkaloid products produced by filamentous cyanobacteria. These products fall into four established subcategories: hapalindoles, ambiguines, fischerindoles, and welwitindoles (45). Some of their notable properties include insecticidal, antibacterial, and antifungal activities. In particular, hapalindoles from *Hapalosiphon fontinalis* are potent inhibitors of fungal species such as *P. notatum*, *Aspergillus oryzae*, and *Candida albicans* (46). Additionally, fischerellin A isolated from *Fischerella muscicola* is a photosystem II inhibitor active against photoautotrophic organisms such as cyanobacteria (47). Structural features of this family of products include a shared indole motif, an isonitrile group, and a monoterpene core. In contrast to IsnA family biosynthesis, indole isonitrile biosynthesis (Figure 1a) is stereoselective for *cis*-configured products (*cis*-**1**) (20). The first terpenoid indole alkaloid, hapalindole A, was isolated in 1984 from cultured *H. fontinalis* (a species of blue-green algae) (48). Further investigation into isonitrile formation in ambiguine NPs revealed biosynthesis from L-tryptophan and ribulose-5-phosphate as the sources of the nitrogen and carbon atoms, respectively. In *F. ambigua* UTEX1903, isonitrile formation is mediated by the *amb* BGC (49). Notably, this cluster contains five genes for tryptophan biosynthesis (*ambT1–5*). The isonitrile synthases AmbI1 and AmbI2 are homologous to IsnA, whereas the Fe(II)/α-KG-dioxygenase AmbI3 is homologous to IsnB. AmbI1 and AmbI3 were sufficient to produce *cis*-**1** (Figure 1a); however, AmbI2/3 were not sufficient for isonitrile production. After synthesis of the indole isonitrile backbone, the monoterpene unit of ambiguine NPs in *F. ambigua* is assembled by the aromatic prenyltransferases FamD1 and FamD2 (50). FamD2 prenylates the indole isonitrile core with geranyl pyrophosphate to yield precursors of tri- and tetracyclic hapalindoles in a pH-dependent manner, whereas FamD1 is a prenyltransferase associated with conjugation of *cis*-**1** with dimethylallyl pyrophosphate (50). These prenyltransferases are notable for their ability to convert between terpenoid isonitrile alkaloid species: FamD1 particularly catalyzes the conversion of tetracyclic hapalindoles to ambiguines. A unique cyclase FamC1 then catalyzes a Cope rearrangement to complete the cyclization of the tetracyclic hapalindole core, resulting in formation of a key alkene intermediate (50). This intermediate is then modified by other pathway/tailoring enzymes to yield various ambiguine derivatives. In *Hapalosiphon welwitschii*, the isonitrile moiety of welwitindole products is synthesized by WelI1–3, which share 93% homology to AmbI1–3 (20). Similarly, in hapalindole biosynthesis, HpiI1–3 were identified as AmbI1–3 homologs.

2.2. Isonitrile Biosynthesis by Fe(II)/α-KG-dioxygenases

The IsnA family of isonitrile synthases was the sole example of an enzyme family dedicated to isonitrile biosynthesis until the discovery of a putative isonitrile lipopeptide (INLP) BGC conserved in many species of *Actinobacteria* (19). The nonribosomal peptide synthetase

(NRPS)-encoding gene cluster (*Rv0096-Rv0101*) from *Mycobacterium tuberculosis* (*Mtb*) was the subject of extensive biological studies supporting the production of a virulence factor; however, the hypothetical metabolite remained elusive (19). Furthermore, in silico homology studies of *Rv0096-Rv0101* revealed five genes (*Rv0097–Rv0101*) conserved among pathogenic *Mycobacteria* and other genera such as *Streptomyces*, *Kutzneria*, *Nocardia*, and *Rhodococcus* (19). The association of this BGC with virulence warranted further metabolomic exploration to understand and establish the function of the five conserved enzymes. Through in vivo reconstitution in *E. coli*, the five genes were found to be necessary and sufficient to produce INLPs similar to the known antibiotic SF2768 (16) (Figure 2a). *Streptomyces coeruleorubidus*, whose *sco* BGC is homologous to the *Mtb* INLP BGC, has been studied as a model for INLP biosynthesis (19). ScoC, an acyl-acyl carrier protein (ACP) ligase, initiates the pathway by activating and loading crotonic acid on ScoB, an acyl carrier protein. ScoD, a thioesterase homolog, then catalyzes a Michael addition of glycine to the β-position of crotonoyl-*S*-ScoB, followed by hydrolysis from the ACP to yield (R)-3-[(carboxymethyl)amino]butanoic acid (CABA). CABA is then subjected to oxidative decarboxylation to yield (R)-3-isocyanobutanoic acid (INBA) by ScoE, a Fe(II)/α-KG-dioxygenase. ScoC acts again in the pathway to activate and load INBA onto ScoB, where the β-isonitrile moiety is condensed by both amino groups of lysine promoted by the single-module NRPS ScoA. The product undergoes a four-electron reductive release from ScoB to form an INLP with a terminal alcohol (19) (Figure 2a).

ScoE's enigmatic reaction is the subject of many recent biochemical, structural, and spectroscopic studies (30, 51–54) to determine its reaction mechanism. We recently conducted in vitro biochemical assays with ScoE to determine the reaction products and stoichiometry (52). Our stoichiometry experiments revealed that two equivalents of α-KG and oxygen are consumed to generate two equivalents of succinate (Figure 2b). One equivalent of CABA was consumed to generate one equivalent of INBA, demonstrating that two α-KG half reactions are required to promote isonitrile formation. Furthermore, an in vitro assay with 6–^{13}C-CABA analyzed with gas chromatography–mass spectrometry further indicated that CO_2 is released from CABA to form INBA (52). Several crystal structures were reported for ScoE both with and without physiological substrates (30, 51, 52). Notably, ScoE contained the archetypal double-stranded β-helix fold from the Fe(II)/α-KG-dioxygenase family with a conserved 2-His-1-Asp carboxylate facial triad responsible for Fe(II) binding. CABA is bound axial to a histidine residue in the carboxylate facial triad, and its carboxylic acid groups interact with Arg310 and Lys193 in the binding pocket, respectively. A comparison between published structures indicated that ScoE may accommodate an inducible α-KG binding site involving a conformational migration of His299 and Arg157 by 10 Å from the surface of the protein to the active site. Biochemical and mutagenesis studies supported the hypothesis that both α-KG half reactions occur within this single inducible binding site and not the offline α-KG binding site observed from our structure with α-KG bound to ScoE.

Fe(II)/α-KG-dioxygenases are known to catalyze various oxidative transformations, such as hydroxylation, epoxidation, halogenation, and ring closure, yet isonitrile formation is a novel transformation requiring a four-electron oxidation of the primary substrate rather than the canonical two-electron oxidations catalyzed by this family. Chang's research group

previously detected a putative C5-OH CABA intermediate by analyzing in vitro enzymatic assays with ScoE homolog SfaA, using 5–^{13}C-CABA and ^{13}C nuclear magnetic resonance to monitor reaction progression by modifying the amount of α-KG. This result was further supported by cocrystallization of the putative C5-OH CABA intermediate bound to ScoE by the same research group. However, C5-OH CABA was not chemically synthesized and tested in vitro to show conversion to INBA. The proposed biosynthetic pathways to isonitrile formation are summarized in Figure 2b (51, 52). Pathways i and ii share a common C5-OH step, whereas pathway iii suggests an initial hydroxylation on the nitrogen atom. Taking pathway I as an example, C5-OH CABA undergoes a subsequent dehydration, and the nitrogen atom is activated by the Fe(IV) = O species to promote oxidative decarboxylation. The resulting formamide or protonated isonitrile then undergoes dehydration or deprotonation, respectively, to yield INBA (52). Pathway ii continues a distinct path with a second hydroxylation at C5, followed by one round of dehydration and a final round of decarboxylation and dehydration to yield INBA (52). Pathway iii proposes N-OH CABA decarboxylation and dehydration, followed by a hydroxylation at C5 and a final dehydration step to generate INBA (52). Though substantial progress has been made to unravel the mechanism for isonitrile formation by Fe(II)/α-KG-dioxygenases, more detailed mechanistic studies remain to be conducted.

2.3. Bioorthogonal Chemistry of Isonitriles and Applications

Isonitriles promote versatile chemistry as nucleophiles and electrophiles owing to their partial carbenoid character, most easily seen in their carbene and zwitterionic representations (8). For example, isonitriles behave as carbon monoxide analogs in regards to metal coordination by participating in π back-bonding with metal atomic orbitals (55) and play an important role as building blocks in chemical synthesis for the development of multicomponent reactions. One key reaction is the Passerini reaction, consisting of isonitrile, carbonyl, and carboxylic acid–containing substrates, and the other is the Ugi reaction, involving the same building blocks and an additional amine substrate. Isonitriles can also function as nucleophiles with halide chlorides to produce reactive chloroiminoketones that yield heterocyclic structures when coupled with an additional ketone-containing chemical substrate (56–58). An important application of the isonitrile functionality is its compatibility for bioorthogonal chemistry in aqueous systems. The two known bioorthogonal reactions involving the isonitrile moiety are covered in this section (Figure 3).

The isonitrile moiety is an ideal candidate for bioorthogonal transformations given its compact structure, stability in biological media (pH 4–9), and ability to be synthesized with relative ease (59). Bioorthogonal reactions occurring under physiological conditions without obstructions from other biological species have important applications in the modification of biomolecules, imaging of NPs/small molecules, nanotechnology, pharmaceutical sciences, and material science (60, 61). The first bioorthogonal reaction was discovered almost four decades ago, when isonitriles were shown to react with tetrazines under physiological conditions to generate a pyrazole motif (62) (Figure 3a). Tetrazines are commonly used substrates for click reactions, with several examples reported with strained alkenes/alkynes for protein-labeling applications (63–65). Isonitrile–tetrazine click reactions commence with a [4+1] cycloaddition reaction, followed by imine formation after release of N_2 and

tautomerization (Figure 3a). When tertiary isonitriles are used, the imine intermediate resists hydrolysis and remains stable in buffered aqueous systems, as demonstrated from metabolic labeling of glycan molecules at the surface of cells (60). However, the imine intermediate from the tetrazine–isonitrile click reaction underwent spontaneous hydrolysis to an aminopyrazole and aldehyde when a primary or secondary isonitrile compound was used, which was an initial roadblock for conjugation reactions owing to the inherent lability of the imine intermediate (60, 61) (Figure 3a). Recent work has leveraged the instability of the imine intermediate for bioorthogonal release reactions (61, 66, 67). Franzini's group synthesized bioorthogonal protecting groups, such as the 3-isocyanopropyl group and tetrazylmethyl derivatives, that can be removed when reacted with tetrazines and isonitriles, respectively (60, 68, 69) (Figure 3b). The application of both bioorthogonal protecting groups has been shown to release two fluorophores in zebrafish (69), a feat that has not been demonstrated from a single bioorthogonal reaction and motivates further studies on bioorthogonal release reactions. Bioorthogonal release reactions may aid in the simultaneous and controlled delivery of multiple synergistic drug combinations (69). Another study aimed to modify the isonitrile–tetrazine click reaction to minimize subsequent hydrolysis of the imine intermediate when a nontertiary isonitrile was used (70). The strategy involved using a solvent panel to find an adequate solvent that would minimize the formation of the aminopyrazole motif to favor reduction of the imine intermediate with $NaBH_3CN$ (Figure 3a). The in situ reduction of the isonitrile–tetrazine click reaction was applied successfully to the extract of a microbial culture expressing *mmaA-E* that is known to produce an INLP with two secondary isonitrile functional groups (19). Liquid chromatography–high-resolution mass spectrometry (LC-HRMS) analysis revealed the expected reduced monoconjugate and diconjugate with 67% reduction efficiency (70).

The isonitrile–tetrazine click reaction not only has extensive applications as a chemical biology tool for labeling biomolecules (60, 62–65, 68, 71, 72) but is an important probe for NP discovery and isonitrile quantification (52, 70, 73, 74). An initial roadblock from the isonitrile–tetrazine click reaction was the spontaneous hydrolysis of the tetrazine–isonitrile conjugate when a primary or secondary isonitrile was used because it restricted the pool of targetable isonitrile substrates (60, 68). Our group recently adapted this unwanted hydrolysis reaction as a tool for rapid and facile isonitrile detection in microbial cultures (70) (Figure 3a). The isonitrile–tetrazine click reaction is a viable discovery tool, because the reaction occurs rapidly under physiological conditions and results in visible color change, serving as an early indicator of isonitrile presence (60, 62). Furthermore, the aminopyrazole motif originating from spontaneous hydrolysis of the isonitrile–tetrazine conjugate can be detected readily using LC-HRMS to indirectly confirm the presence of an isonitrile metabolite (Figure 3a). A thorough kinetic analysis of the click reaction demonstrated complete conversion of several synthetic isonitrile compounds (1 mM) within 1 h when tetrazine was added in 10× excess (1:1 MeOH:H_2O), suggesting these conditions can be applied to quantify up to 1 mM of isonitrile in a microbial culture. Notably, the reaction mixture changed from bright red/pink to light yellow as tetrazine was converted to aminopyrazole. The tetrazine–isonitrile click reaction was then used to detect and quantify isonitrile metabolites produced by *E. coli* heterologous expression strains expressing *scoA-E* and the homologous BGC *mmaA-E*, which were previously constructed by our group (19,

70). After addition of tetrazine to the culture extracts, an immediate color change was observed with concomitant production of the aminopyrazole motif, which was not observed from an empty vector control (70). Importantly, known INLPs produced by the heterologous expression strains were not detected after the click reaction, suggesting complete conversion of the isonitrile metabolites. INLP titer was estimated by generating a calibration curve for the aminopyrazole motif with LC-HRMS (70). Using this strategy, we also quantified the amount of INBA produced from an in vitro ScoE reaction and demonstrated that CABA consumption is stoichiometric with INBA production (52).

Our group also applied the isonitrile–tetrazine click reaction to discover novel isonitrile-containing NPs from candidate producers through genome mining. Our bioinformatic analyses revealed a homologous *scoA-E* gene cluster in *Streptomyces tsukubaensis* NRRL 18488, a known producer of nonisonitrile NPs tacrolimus (FK506) and triacsins (75–77). A color change in the tetrazine reaction mixture incubated with culture extracts indicated presence of an isonitrile-containing compound. LC-HRMS analysis also identified a candidate metabolite that disappeared after the click reaction (70). The isonitrile–tetrazine click reaction was also used to screen for isonitrile-containing NPs from *Mtb* biofilms. Metabolomic comparison between planktonic and biofilm *Mtb* cultures and *Mtb* Δ*Rv0096-Rv0101* (Δ*inlp*) revealed four candidate metabolites present in biofilm cultures but not planktonic cultures or the Δ*inlp* strain (74). Subsequent addition of tetrazine resulted in the detection of aminopyrazole and disappearance of the four metabolites, suggesting all four bear the isonitrile functionality (74). Crawford's research group (73) also used the isonitrile–tetrazine click reaction to demonstrate intermediacy of an isonitrile-containing compound from the *N*-acyl-L-histidine biosynthetic pathway in *L. pneumophila*. These examples support the isonitrile–tetrazine click reaction as a robust, facile tool to expedite discovery of isonitrile-containing NPs.

The second click reaction of interest is the bioorthogonal isonitrile–chlorooxime reaction, a rapid ligation [k = 1 1/(M*s)] reaction yielding a hydroxyimino amide product (59) (Figure 3c). Chlorooximes are known to react with isonitriles in various organic solvents to yield α-hydroxyimino amides, a small functionality ideal for ligation reactions. Wennemer's research group postulated that a similar reaction may occur in an aqueous system through water-assisted production of a nitrile oxide species from the chlorooxime (Figure 3c). The nitrile oxide species then reacts with an isonitrile-containing molecule to yield a reactive nitrilium ion that gets hydrolyzed to yield the desired α-hydroxyimino amide (59) (Figure 3c). The group further demonstrated that performing the reaction in aqueous media was essential for activity, and the rate was enhanced at 37°C relative to room temperature. Reaction chemoselectivity was next probed through competition experiments using common biologically relevant functional groups, such as carboxylic acids, amines, amides, imidazole, alcohols, and alkenes. Thiols originating from glutathione were the only functionality shown to interfere with the reaction, but chemoselectivity was restored when the reaction was performed at pH 5 compared to physiological pH. The isonitrile–chlorooxime ligation reaction was further applied to metabolic labeling of cell-surface glycans with *N*-acetylmannosamines. Furthermore, the isonitrile–chlorooxime reaction was shown to be compatible alongside the azide–alkyne click reaction from a live-cell imaging

experiment that ultimately highlighted their orthogonality and prospective use in dual-labeling experiments (59).

2.4. Engineering the Biosynthesis of Isonitriles

The isonitrile moiety is an intriguing functionality linked to various bioactivities (14–16), while also playing a prominent role as a building block in organic synthesis and bioorthogonal reactions in chemical biology applications (56, 60, 63, 71). Yet, the advances toward employing isonitrile biosynthetic machinery to produce novel isonitrile-containing biomolecules remain limited (19, 78, 79). This section aims to provide prospects and advances toward employing characterized biosynthetic machinery to generate isonitrile-functionalized small molecules.

Hapalindoles are a large family of NPs containing cytotoxic activities toward multidrug-resistant bacteria, fungi, and human tumor cells (78). Liu's research group aimed to explore the promiscuity of the isonitrile machinery from the hapalindole biosynthetic pathway (Amb1–3) in incorporating unnatural functionalities such as halogens into cytotoxic hapalindoles to improve bioactivity and bioavailability to further enable potential cross-coupling chemistry (78). F-substitution across carbon atoms 4–7 (C4–C7) of L-tryptophan was successfully recognized by the Amb1–3 machinery in vitro and generated the corresponding F-substituted *cis*-indolyl vinyl isonitriles with comparable efficiency to unmodified L-tryptophan. The effect of halogen substitution at C5 or C7 using chlorine, bromine, or iodine revealed decreasing levels of conversion as halogen size increased (78). Liu's research group next investigated the ability to produce halo-substituted indole vinyl isonitriles through heterologous expression of *amb1–3* in *E. coli*, which resulted in successful detection of F-substituted *cis*-indolyl vinyl isonitriles when the corresponding F-substituted L-tryptophan substrates were fed. Further optimization of the feeding concentrations resulted in a titer of 0.6 mg/L of 6-F *cis*-indolyl vinyl isonitrile, highlighting the viability of the expression system (78). Viswanathan's research group employed a similar strategy with the homologous WelI1–3 biosynthetic machinery to convert eight L-tryptophan-derived α-amino acids (methylation, *O*-methylation, and halogenation on the side chain) to their corresponding isonitrile compounds, which further expanded the enzymatic promiscuity of the biosynthetic machinery (79).

Our characterization of the INLP pathway in *Actinobacteria* revealed important insight into the substrate specificity for the enzymes involved in their biosynthesis and opened the door for potential engineering applications (19). The acyl-ACP ligases from *Streptomyces coelureorubidus* (ScoC) and *Mycobacterium marinum* (MmaC) were subjected to ATP-[^{32}P]PP$_i$ exchange assays to determine their substrate preference. The ATP-[^{32}P]PP$_i$ exchange assay is a classic assay used to characterize the substrate specificity of adenylating enzymes by using liquid scintillation counting to measure the amount of ATP-[^{32}P]PP$_i$ absorbed to a charcoal suspension that was produced from the reversible adenylation reaction when [^{32}P]PP$_i$ is added. ScoC proved to preferentially activate fatty acids with a carbon chain length between 4 and 8. However, direct substrate activation and loading assays of MmaC revealed preferential activation of medium-chain-length fatty acids (>C8) (19). This result aligns with biochemical and structural analysis of Rv0099, a

homolog of MmaC from *Mtb*, that demonstrated activation of medium-chain-length fatty acids (80, 81). Both proteins also demonstrated tolerance toward α,β-unsaturated fatty acids. These results suggest that ScoE homologs have different chain-length specificity. Furthermore, the NRPSs ScoA and MmaA preferentially activate L-lysine but tolerate D-lysine. Although L-ornithine was not recognized by ScoA/MmaA, it may be a preferred substrate for other conserved NRPSs based on the chemical structure of SF2369 (19, 44). Based on the substrate preference for the acyl-ACP ligases in the same INLP operon, it is conceivable to test CABA analogs to determine whether ScoE and its homologs can convert these substrates to INBA analogs. Together with the promiscuous NRPSs encoded in the operon, the INLP biosynthetic pathway in *Actinobacteria* is prospective for generating diverse isonitrile-bearing small molecules.

3. ALKYNE BIOSYNTHESIS AND ENGINEERING

Acetylenic NPs containing terminal alkynes are widespread metabolites in plants, fungi, marine sponges, and insects (10, 13, 82, 83). Only two enzyme classes are known to form the terminal alkyne moiety: first, JamB-like nonheme diiron desaturases/acetylenases, and second, BesB-like PLP-dependent lyases (84, 85) (Figure 4). Despite the known mechanisms, the biosynthesis of many NPs endowed with a terminal alkyne moiety remains unknown (10). Additionally, biosynthetic routes for some internal alkyne-containing or polyynyl NPs are known but are not reviewed here (10).

Selective installation of an alkyne moiety is a key goal in biomolecular engineering because of the alkyne's usefulness as a pharmacophore and in bioorthogonal chemistry approaches, among other applications (86, 87). This motivation has sparked advances in de novo biosynthesis of alkyne-labeled NPs, improvements in terminal alkyne biosynthetic machinery, and development of new bioorthogonal chemistry approaches for studying molecular function in vivo (88). Here, we discuss known alkyne biosynthesis mechanisms, prospects for using the alkyne in the study of biologically relevant small molecules, and advances in engineering alkyne biosynthesis.

3.1. Biosynthesis of the Terminal Alkyne Functionality by JamB

JamB is a nonheme diiron membrane-bound bifunctional desaturase/acetylenase that generates a terminal alkyne, instead of an internal alkyne like Crep1 (84). In the biosynthesis of cyanobacterial NP jamaicamide B, JamB was discovered to be essential for the formation of a terminal alkyne functionality. JamB is encoded in a tri-gene cassette alongside an acyl-ACP synthetase, JamA, and an ACP, JamC (84) (Figure 4a). These three proteins comprise an ACP-dependent pathway to generate the terminal alkyne functionality: JamA activates and loads hexanoic acid onto JamC, and JamB modifies the resulting hexanoyl-*S*-JamC to yield 5-hexynoyl-*S*-JamC as a starter unit for the downstream polyketide synthase (PKS)/NRPS assembly line (84) (Figure 4a). Through both in vitro and in vivo analyses, JamB was demonstrated to be a carrier protein–dependent membrane-bound acetylenase/desaturase with stringent substrate specificity toward both the acyl group and the acyl carrier (84).

A detailed mechanistic investigation of JamB remains elusive given the inherent difficulties in expressing soluble membrane-bound proteins. JamB stands out from canonical

desaturases/acetylenases for a few reasons. First, membrane-bound desaturases most commonly accept acyl-CoA or glycerolipid substrates, but an ACP-conjugated substrate is needed for JamB activity. Second, how JamB abstracts two hydrogens from adjacent carbons linked by a double bond without forming an epoxide is not understood. The structure of SCD1, a membrane delta 9 desaturase sharing a similar diiron center with JamB, was recently solved with two iron ions bound (89, 90). The Zhou group reconstituted the activity of SCD1 in vitro with NADPH, cytochrome b5 reductase, and cytochrome b5. Despite differences between SCD1 and JamB, the crystal structure of SCD1 serves as a viable model to probe further mechanistic understanding of JamB.

Our previous genome-mining work also revealed a homologous tri-gene cassette encoding TtuA, TtuB, and TtuC, which were biochemically characterized and compared with their homologs (91) (Figure 4a). The major difference between JamB and TtuB is the substrate specificity. JamB prefers C6 fatty acids, whereas TtuB prefers C10 fatty acids. The TtuABC pathway echoes JamABC; TtuA activates and loads decanoic acid onto TtuC, then the decanoyl-*S*-*TtuC* is modified by TtuB to produce 9-decynoyl-*S*-TtuC (91) (Figure 4a).

3.2. Alkynyl Amino Acid Biosynthesis

Among the thousands of acetylenic compounds Nature produces are a handful of alkynyl amino acids bearing the terminal alkyne moiety, including propargylglycine, ethynylglycine, and β-ethynylserine (92–94). All three compounds are produced by *Streptomyces* spp., and some have been established as antimetabolites (85, 93). Although alkynyl amino acids have been known for decades, researchers have started to elucidate their biosynthetic origins only recently.

β-Ethynylserine, a product of *Streptomyces cattleya*, was incidentally isolated during bioactivity-guided fractionation of another threonine antimetabolite, 4-fluorothreonine (93, 95). Recognizing that protein and proteome labeling through indigenously produced rather than synthetic terminal alkyne-containing amino acids could facilitate advances in chemical biology, Marchand et al. (85) sought to identify the genomic underpinnings for β-ethynylserine biosynthesis. Disruption of predicted fatty acid desaturases in *S. cattleya* did not impact β-ethynylserine production (85). A comparative genomics approach using the two known β-ethynylserine producers, *S. cattleya* and *Streptomyces catenulae*, and the genomes of 26 nonproducing *Streptomyces* spp. revealed a five-gene biosynthetic cassette with predicted functions associated with amino acid biosynthesis (85).

This five-gene biosynthetic cassette was targeted for gene disruption in *S. cattleya*, and deletion of four genes, *besB–E*, abrogated β-ethynylserine production (85) (Figure 4b). Deletion of *besB–D* eliminated propargylglycine, but the Δ*besE* strain still produced propargylglycine, suggesting BesE is a hydroxylase that converts propargylglycine to β-ethynylserine, confirming the in silico prediction (85) (Figure 4b). Based on comparative metabolomic evidence from the gene disruption strains and wild-type *S. cattleya*, the biosynthetic pathway for β-ethynylserine was proposed to commence from an L-lysine precursor, which was confirmed through in vitro reconstitution (85) (Figure 4b). First, L-lysine is chlorinated at Cγ by BesD, a nonheme Fe(II) and α-KG-dependent halogenase. The activity of BesD has since been supported through additional structural studies (96).

BesC then cleaves 4-Cl-lysine to form 4-Cl-allylglycine, the chloride of which is then eliminated by BesB, a PLP-dependent enzyme, to form propargylglycine (85). BesA acts next in the pathway to ligate L-glutamate to propargylglycine in an ATP-dependent manner, followed by hydroxylation at C_β by BesE (85). An unknown enzyme releases the glutamyl prosthetic, yielding β-ethynylserine (85).

3.3. The Study and Harnessing of Terminal Alkynes in Bioorthogonal Chemistry

Over the past two decades, bioorthogonal chemistry has emerged as a promising suite of methods to probe biological function (97, 98). The terminal alkyne has emerged as a strong candidate in bioorthogonal chemistry applications for several reasons: Terminal alkynes are rare in Nature, minimally disruptive to molecular function, stable, and robustly clickable, particularly through the highly chemoselective Cu(I)-dependent azide–alkyne cycloaddition, enabling creative tagging strategies for small molecules and biological macromolecules alike (86, 99) (Figure 5a). This promise has only increased as the fundaments of alkyne biogenesis have been revealed and harnessed.

Zhu et al. (100) creatively employed click chemistry to report JamB activity. JamB, though a promising tool in biomolecular engineering, only weakly converts alkyl substrates to the terminal alkyne in *E. coli*, meriting protein engineering to improve in vivo efficiency. To quickly assess JamB engineering outcomes, Zhu et al. (100) developed a novel screening method based on the quantification of alkyne-tagged metabolites directly in their producing cell cultures. This platform has two components: first, tagging of HsPKS1-produced polyketides with a hexynoyl moiety furnished by JamABC, followed by a Cu(I)-dependent click reaction with an azido fluorogenic probe to identify the secreted, tagged polyketides (100) (Figure 5a,b). Fluorescence of the unmodified probe is quenched, but the probe-target complex fluoresces readily, permitting fluorescence enhancement as a readout for alkyne concentration (100). This strategy facilitated directed evolution of a JamB variant library, revealing a few amino acid residues as gatekeepers of JamB activity (100). Notably, these include M5 and I23; mutating these residues conferred greater activity than wild-type JamB. JamB-M5T was shown to have 20-fold greater activity than wild-type JamB in *E. coli* (100). Therefore, this strategy not only yields a more efficient JamB variant for applications in an *E. coli* background but contributes to a mechanistic understanding of JamB activity.

The ability to report the presence of the alkyne moiety against a complex metabolomic background through alkyne–azide click chemistry has enabled deployment of azide probes to identify and purify alkynyl NPs and intermediates (12, 101). For example, the use of a hybrid fluorescence and mass probe facilitated discovery of vatiamide congeners (101). The vatiamides, which share many structural traits with the jamaicamides, including the coveted terminal alkyne and vinyl chloride moieties, were isolated from marine cyanobacteria through a bioactivity-guided fractionation approach (101). To identify hypothetical vatiamide congeners, Moss et al. (101) screened crude extracts from known vatiamide producers using a coumarin-based fluorescence probe bearing a bromine atom, enabling both fluorescence and mass spectrometric readouts. This strategy spotlighted vatiamides E and F, whose presence suggested a combinatorial biosynthetic route (101). Additionally, the azide–alkyne cycloaddition has been used to stabilize the terminal alkyne

moiety in highly unstable polyynyl compounds. Specifically, benzyl azide probes trapped key intermediates in caryoynencin, protegenin, and collimonin biosynthesis, helping to elucidate their respective biosynthetic pathways (102–104).

Small-molecule tagging for Raman imaging is a particularly promising approach for studying small-molecule function in vivo (7). In addition to the chemical properties of alkynes that heighten their promise in all bioorthogonal applications, alkynes possess a unique Raman peak in a cell-silent spectral region (7). Thus, live cell imaging experiments are possible using a Raman spectroscopy approach with a very simple and small alkyne tag. Indeed, alkyne-functionalized primary metabolites, including fatty acids, steroids, sugars, and nitrogenous bases, have been imaged successfully using a Raman approach (105–110).

The bioactivity of small-molecule NPs has been studied through the installation of bioorthogonal handles, including terminal alkyne and azide moieties, by modifying NP scaffolds through synthesis or semisynthesis, as in recent antimycin structure–activity–distribution studies (88, 108). However, the need for a synthetic or semisynthetic route is a major barrier to scalable application of this method. As an alternative, bioorthogonal functionalization through precursor-directed biosynthesis (PDB) relies on incorporation of the bioorthogonal handle through native or engineered biosynthetic machinery (88). Despite successes with introducing an alkynyl handle to NP scaffolds in this manner (111, 112), PDB suffers from high background, motivating pathway-level strategies to incorporate a bioorthogonal handle during committed steps of target biosynthesis. To this end, JamABC is a promising tool for functionalization of target NPs (88). We await further studies leveraging the JamABC tool kit for in vivo installation of an alkyne handle (88, 113).

Since the advent of bioorthogonal noncanonical amino acid tagging, the exogenous application of alkynyl amino acids, especially propargylglycine and homopropargylglycine, coupled with click chemistry–mediated tagging, has advanced knowledge of protein function in vivo (87). Protein tagging can proceed in site- or residue-specific manners (114). Often, the noncanonical amino acid is introduced by an engineered transfer RNA synthetase. Site-specific tagging proceeds through leveraging co-opted amber stop codons, whereas residue-specific tagging leverages the START codon, replacing methionine residues, or depleted codons (114). Recognizing the potential utility of biologically produced propargylglycine, Marchand et al. (85; see also 115, 116) labeled the *E. coli* proteome with propargylglycine by co-expressing BesBCD with PraRS, a propargylglycine-tolerant metRS derivative, and the chaperonins GroEL-GroES, enabling fluorescence imaging once conjugated with an azido fluorescence tag.

3.4. Advances in Engineered Production of Alkynyl Biomolecules

Elucidation of alkynyl biosynthetic machinery has enabled advances in the production of novel biomolecules bearing a terminal alkyne moiety. As a proof of principle, the *jamABC* cassette for terminal alkyne biosynthesis was repurposed to endow PK scaffolds with an alkynyl moiety (84). To demonstrate the potential of JamABC as a tool to generate terminal alkyne-tagged biomolecules, Zhu et al. (84; see also 117, 118) turned to HsPKS1, a type III PKS with unusually broad substrate tolerance toward both acyl groups and acyl carriers of the starter unit (Figure 5b). Zhu et al. (84, 91) demonstrated incorporation of a hexynoyl

moiety as a starter unit into a novel pyrone scaffold through co-expression of *hspks1* and the *jamABC* cassette in an *E. coli* BAP1 host, advancing HsPKS1 as a candidate in vivo reporter system for terminal alkyne biosynthesis. Indeed, co-expression of *hspks1* along with several cassettes homologous to *jamABC* revealed novel terminal alkyne biosynthesis machinery (91). Many additional promiscuous type III PKSs are expected to take an alkynyl starter unit generated from JamABC or its homologous biosynthetic machinery.

An important advancement toward optimizing the *jamABC* tool kit was established by probing the protein–protein interactions within the terminal alkyne biosynthetic machinery. Our research group determined that JamB interacts stringently with its cognate ACP (JamC) (119), as noncognate ACPs led to no or significantly less production of alkyne product. A protein engineering approach was employed to change the electrostatic surfaces of noncognate ACPs to improve their interactions with JamB. Structural comparisons between JamC and TtuC revealed a positively charged eight–amino acid region that was present in helix 3 of TtuC but was not present in JamC. A K69T mutation of TtuC within this amino acid region resulted in an engineered strain with comparable efficiency to JamC in generating a terminal-alkyne tagged PK. Notably, the mutation had no effect on TtuC expression or recognition by JamA, thus suggesting improved interactions between JamB and K69T TtuC. Error-prone mutagenesis was used to generate a library of PeACP variants that revealed additional hotspots for ACP engineering in helices 2 and 3, resulting in 16-fold-improved activity compared to the wild-type peACP strain (119).

Our recent work on the de novo biosynthesis of terminal alkyne-tagged PKs by engineered modular type I PKSs (LipPKS1 and DEBSM6) highlighted two engineering strategies to improve ACP-ketosynthase (KS) interactions (120) (Figure 5c). A terminal alkyne-tagged PK was detected successfully in vitro when the engineered PKSs were incubated with 5-hexynoyl-*S*-JamC that was synthesized in situ, suggesting that 5-hexynoyl-*S*-JamC could also serve as a starter unit for engineered type I PKSs. It was hypothesized that improving the communication between upstream JamC and the downstream KS could lead to more efficient alkyne-tagged PK biosynthesis because protein–protein interactions are known to control turnover of chimeric PKS assembly lines (120). Alkyne tagging efficiency was improved substantially by fusing the portable docking domains from the curamycin biosynthetic pathway, $_{C}dd^{CurK}$ and $_{N}dd^{CurL}$, with JamC and both engineered PKSs, respectively (120–122) (Figure 5c). Importantly, poor production of alkyne-tagged PK with the docking domain fused to only JamC excluded the possibility of improved recognition of modified JamC by JamA, indicating that improved communication between engineered JamC and KS was due to the docking domain strategy. In addition, site-directed mutagenesis of a key residue contributing to chain translocation specificity within helix 1 of JamC (E32) was employed to improve ACP–KS protein–protein interactions, exemplified by increased production of terminal alkyne-tagged PKs (sevenfold for LipPKS1* and twofold for DEBSM6*). The in vitro experiments that employed protein engineering demonstrated the success in enhancing recognition of JamC by the PKSs to promote translocation of the alkyl unit. However, it was unclear whether the JamC modifications would impact JamB activity, motivating further in vivo experiments (120). The production of terminal-alkyne-tagged PKs was quantified from in vivo expression of *jamABC* and PKSs, along with their engineered variants in *E. coli BAP1* cultures fed with 5-hexenoic acid. The

ratio of alkyne/alkene PK was found to be approximately 1:5 using LipPKS1* with a fourfold drop when either docking domain pair was used. This result suggested that modification of JamC affected its recognition by JamB. However, use of E32T JamC increased the titer of alkyne by sixfold, because helix 1 does not interact with JamB (84, 119) (Figure 5c). Implementation of the docking domain strategy and site-directed mutagenesis individually and synergistically revealed significantly improved production of terminal alkyne-tagged PKs. The protein engineering strategy for de novo biosynthesis of alkyne-tagged polyketides was successful, yet there are limitations and considerations for future engineering applications. The strategy is currently limited to incorporation of an alkynyl unit, which must be tolerated by PKSs. Alkynyl incorporation is expected to be challenging for PKSs that recognize very different starter units, including DEBSM6* that exhibited poor efficiency in vivo owing to the complex metabolic background (120). We eagerly await future discovery of JamABC homologs that yield various alkynyl substrates that may serve as starter units to expand the repertoire of alkyne-tagged PKs.

Although most PKs are extended by malonyl-CoA or methylmalonyl-CoA subunits (123), incorporation of alkyne-containing malonyl-CoA analogs could permit alkyne tagging through extender unit engineering. The antimycin-type depsipeptides have been identified as promising candidates for alkynyl tagging owing to the broad alkyl substrate scope permitted by AntE, a promiscuous reductase/carboxylase that fashions precursors for the PKS AntD (111, 124, 125). PDB experiments revealed that a stunning diversity of fatty acyl extender units, including alkynyl substrates, can be incorporated in the antimycin scaffold (111). To couple with de novo alkynyl extender unit biosynthesis, Zhu et al. (84) targeted antimycin for alkynylation by co-expressing the minimum set of genes for antimycin biosynthesis (*antCDEFGM*) with *jamABC* in *E. coli* BAP1. Alkyne-tagged antimycin type metabolites were produced successfully, albeit at a very low efficiency (84). Though substantial advances have yet to be made in optimizing routes for alkynyl extender unit incorporation through pathway engineering, the successful alkynylation of the antimycin scaffold represents a promising step toward site-specific introduction of the terminal alkyne in other systems.

4. CONCLUSION

NPs are rich sources for bioactive small molecules with extensive applications to therapeutics, commodity chemicals, and biological probes. These properties are commonly imparted from the array of functional groups that decorate these specialized metabolites. The isonitrile and terminal alkyne are two unusual functional groups whose biosynthetic pathways were discovered in the last decade. A thorough understanding of their biosynthetic pathways is vital to the scientific community for four reasons. First, the underlying biosynthesis of unusual functional groups contributes to fundamental enzymology, allowing rigorous mechanistic studies to afford these functionalities. Second, both groups contain clickable functionalities that enable bioorthogonal reactions that may aid in the discovery of novel NPs and in probing biological functions of small molecules. Third, biosynthetic pathways for these functionalities are attractive targets for virulence attenuation and harnessing of antimicrobial molecules. Fourth, engineering of their biosynthetic machinery was successful in incorporating clickable functional groups to synthesize tagged NPs. The

advances made in understanding how terminal alkynes and isonitriles are synthesized in Nature will pay dividends as they are developed into potent biocatalysts to produce value-added chemicals in the future.

ACKNOWLEDGMENTS

The relevant research in the Zhang lab was financially supported by grants to W.Z. from the National Institute of Health (R01GM136758 and DP2AT009148), the American Cancer Society (Grant RSG-17-013-01-CDD), and the Chan Zuckerberg Biohub Investigator Program.

LITERATURE CITED

1. Li JS, Barber CC, Zhang W. 2019. Natural products from anaerobes. J. Ind. Microbiol. Biotechnol. 46(3–4):375–83 [PubMed: 30284140]
2. O'Brien J, Wright GD. 2011. An ecological perspective of microbial secondary metabolism. Curr. Opin. Biotechnol. 22(4):552–58 [PubMed: 21498065]
3. Romero D, Traxler MF, López D, Kolter R. 2011. Antibiotics as signal molecules. Chem. Rev. 111(9):5492–505 [PubMed: 21786783]
4. Newman DJ, Cragg GM. 2016. Natural products as sources of new drugs from 1981 to 2014. J. Nat. Prod. 79(3):629–61 [PubMed: 26852623]
5. Ren Y, Bai Y, Zhang Z, Cai W, Del Rio Flores A. 2019. The preparation and structure analysis methods of natural polysaccharides of plants and fungi: a review of recent development. Molecules 24(17):3122 [PubMed: 31466265]
6. Skyrud W, Del Rio Flores A, Zhang W. 2020. Biosynthesis of cyclohexanecarboxyl-CoA highlights a promiscuous shikimoyl-CoA synthetase and a FAD-dependent dehydratase. ACS Catal. 10(5):3360–64
7. Wei L, Hu F, Shen Y, Chen Z, Yu Y, Lin C, et al. 2014. Live cell imaging of alkyne-tagged small biomolecules by stimulated Raman scattering. Nat. Methods 11(4):410–12 [PubMed: 24584195]
8. Zhang X, Evanno L, Poupon E. 2020. Biosynthetic routes to natural isocyanides. Eur. J. Org. Chem. 2020(13):1919–29
9. Chen T-Y, Chen J, Tang Y, Zhou J, Guo Y, Chang W-C. 2021. Current understanding toward isonitrile group biosynthesis and mechanism. Chin. J. Chem. 39(2):463–72 [PubMed: 34658601]
10. Li X, Lv J, Hu D, Abe I. 2021. Biosynthesis of alkyne-containing natural products. RSC Chem. Biol. 2:166–80 [PubMed: 34458779]
11. Haritos VS. 2015. A terminal triple bond toolbox. Nat. Chem. Biol. 11:98–99 [PubMed: 25531892]
12. Zhu X, Zhang W. 2018. Terminal alkyne biosynthesis in marine microbes. Methods Enzymol. 604:89–112 [PubMed: 29779667]
13. Minto RE, Blacklock BJ. 2008. Biosynthesis and function of polyacetylenes and allied natural products. Prog. Lipid Res. 47:233–306 [PubMed: 18387369]
14. Clarke-Pearson MF, Brady SF. 2008. Paerucumarin, a new metabolite produced by the *pvc* gene cluster from *Pseudomonas aeruginosa*. J. Bacteriol. 190(20):6927–30 [PubMed: 18689486]
15. Crawford JM, Portmann C, Zhang X, Roeffaers MBJ, Clardy J. 2012. Small molecule perimeter defense in entomopathogenic bacteria. PNAS 9(27):10821–26
16. Wang L, Zhu M, Zhang Q, Zhang X, Yang P, Liu Z, et al. 2017. Diisonitrile natural product sf2768 functions as a chalkophore that mediates copper acquisition in *Streptomyces thioluteus*. ACS Chem. Biol. 12(12):3067–75 [PubMed: 29131568]
17. Gloer JB, Rinderknecht BL. 1989. Nominine: a new insecticidal indole diterpene from the sclerotia of *Aspergillus nomius*. J. Org. Chem. 1989(6):2530–32
18. Lim FY, Won TH, Raffa N, Baccile JA, Wisecaver J, et al. 2018. Fungal isocyanide synthases and xanthocillin biosynthesis in *Aspergillus fumigatus*. Am. Soc. Microbiol. 9(3):e00785–18

19. Harris NC, Sato M, Herman NA, Twigg F, Cai W, Liu J, et al. 2017. Biosynthesis of isonitrile lipopeptides by conserved nonribosomal peptide synthetase gene clusters in Actinobacteria. PNAS 114(27):7025–30 [PubMed: 28634299]
20. Hillwig ML, Zhu Q, Liu X. 2014. Biosynthesis of ambiguine indole alkaloids in cyanobacterium *Fischerella ambigua*. ACS Chem. Biol. 9(2):372–77 [PubMed: 24180436]
21. Soledade MSC, Yaya EE. 2012. The first isocyanide of plant origin expands functional group diversity in cruciferous phytoalexins: synthesis, structure and bioactivity of isocyalexin A. Org. Biomol. Chem. 10:3613–16 [PubMed: 22495624]
22. Emsermann J, Kauhl U, Opatz T. 2016. Marine isonitriles and their related compounds. Mar. Drugs 14(1):16 [PubMed: 26784208]
23. Schnermann MJ, Shenvi RA. 2016. Syntheses and biological studies of marine terpenoids derived from inorganic cyanide. Nat. Prod. Rep. 32(4):543–77
24. Manzo E, Ciavatta ML, Gavagnin M, Mollo E, Guo Y-W, Cimino G. 2004. Isocyanide terpene metabolites of *Phyllidiella pustulosa*, a nudibranch from the South China Sea. J. Nat. Prod. 2004:1701–4
25. Karuso P, Scheuer PJ. 1989. Biosynthesis of isocyanoterpenes in sponges. J. Org. Chem. 54(9):2092–95
26. Garson MJ, Simpson JS, Flowers AE, Dumdei EJ. 2000. Cyanide and thiocyanate-derived functionality in marine organisms - structures, biosynthesis and ecology. Stud. Nat. Prod. Chem. 21:329–72
27. Fookes CJR, Garson MJ, MacLeod JK, Skelton BW, White AH. 1988. Biosynthesis of diisocyanoadociane, a novel diterpene from the marine sponge *Amphimedon* sp. crystal structure of a monoamide derivative. J. Chem. Soc. Perkins Trans. 1:1003–11
28. Garson MJ. 1986. Biosynthesis of the novel diterpene isonitrile diisocyanoadociane by a marine sponge of the *Amphimedon* genus: incorporation studies with sodium [^{14}C]cyanide and sodium [2-^{14}C]acetate. J. Chem. Soc. Chem. Commun. 1986:35–36
29. Brady SF, Clardy J. 2005. Cloning and heterologous expression of isocyanide biosynthetic genes from environmental DNA. Angew. Chem. 44(43):7063–65 [PubMed: 16206308]
30. Harris NC, Born DA, Cai W, Huang Y, Martin J, Khalaf R, et al. 2018. Isonitrile formation by a non-heme iron(II)-dependent oxidase/decarboxylase. Angew. Chem. Int. Ed. 57(31):9707–10
31. Brady SF, Chao CJ, Handelsman J, Clardy J. 2001. Cloning and heterologous expression of a natural product biosynthetic gene cluster from eDNA. Org. Lett. 3(13):1981–84 [PubMed: 11418029]
32. Brady SF, Chao CJ, Clardy J. 2002. New natural product families from an environmental DNA (eDNA) gene cluster. J. Am. Chem. Soc. 124:9968–69 [PubMed: 12188643]
33. Brady SF, Clardy J. 2004. Palmitoylputrescine, an antibiotic isolated from the heterologous expression of DNA extracted from bromeliad tank water. J. Nat. Prod. 67:1283–86 [PubMed: 15332842]
34. Brady SF, Chao CJ, Clardy J. 2004. Long-chain *N*-acyltyrosine synthases from environmental DNA. Appl. Environ. Microbiol. 70(11):6865–70 [PubMed: 15528554]
35. Brady SF, Clardy J. 2000. Long-chain *N*-acyl amino acid antibiotics isolated from heterologously expressed environmental DNA. J. Am. Chem. Soc. 122:12903–4
36. Brady SF, Clardy J. 2005. Systematic investigation of the *Escherichia coli* metabolome for the biosynthetic origin of an isocyanide carbon atom. Angew. Chem. Int. Ed. 44:7045–48
37. Chang W-c, Sanyal D, Huang J-L, Ittiamornkul K, Zhu Q, Liu X. 2017. In vitro stepwise reconstitution of amino acid derived vinyl isocyanide biosynthesis: detection of an elusive intermediate. Org. Lett. 19:1208–11 [PubMed: 28212039]
38. Drake EJ, Gulick AM. 2008. Three-dimensional structures of *Pseudomonas aeruginosa* PvcA and PvcB, two proteins involved in the synthesis of 2-isocyano-6,7-dihydroxycoumarin. J. Mol. Biol. 384(1):193–205 [PubMed: 18824174]
39. Rothe W 1954. Das neue Antibiotikum Xanthocillin. Dtsch. Med. Wochenschr. 79:1080–81 [PubMed: 13182909]

40. Briza P, Eckerstorfer M, Breitenbach M. 1994. The sporulation-specific enzymes encoded by the DITI and DIT2 genes catalyze a two-step reaction leading to a soluble LL-dityrosine-containing precursor of the yeast spore wall. PNAS 91:4524–28 [PubMed: 8183942]
41. Qaisar U, Luo L, Haley CL, Brady SF, Carty NL, et al. 2013. The *pvc* operon regulates the expression of the *Pseudomonas aeruginosa* fimbrial chaperone/usher pathway (Cup) genes. PLOS ONE 8(4):e62735 [PubMed: 23646138]
42. Qaisar U, Kruczek CJ, Azeem M, Javaid N, Colmer-Hamood JA, Hamood AN. 2016. The *Pseudomonas aeruginosa* extracellular secondary metabolite, Paerucumarin, chelates iron and is not localized to extracellular membrane vesicles. J. Microbiol. 54(8):573–81 [PubMed: 27480638]
43. Oh J, Kim NY, Chen H, Palm NW, Crawford JM. 2019. An Ugi-like biosynthetic pathway encodes bombesin receptor subtype-3 agonists. J. Am. Chem. Soc. 141(41):16271–78 [PubMed: 31537063]
44. Dose B, Niehs SP, Scherlach K, Shahda S, Flórez LV, et al. 2021. Biosynthesis of sinapigladioside, an antifungal isothiocyanate from *Burkholderia* symbionts. ChemBioChem 22(11):1920–24 [PubMed: 33739557]
45. Raveh A, Carmeli S. 2007. Antimicrobial ambiguines from the cyanobacterium *Fischerella* sp. collected in Israel. J. Nat. Prod. 70(2):196–201 [PubMed: 17315959]
46. Smitka TA, Bonjouklian R, Doolin L, Jones ND, Deeter JB, Yoshida WY, et al. 1992. Ambiguine isonitriles, fungicidal hapalindole-type alkaloids from three genera of blue-green algae belonging to the Stigonemataceae. J. Org. Chem. 57(3):857–61
47. Hagmann L, Jüttner F. 1996. Fischerellin A, a novel photosystem-II-inhibiting allelochemical of the cyanobacterium *Fischerella muscicola* with antifungal and herbicidal activity. Tetrahedron Lett. 37(36):6539–42
48. Moore RE, Cheuk C, Patterson GML. 1984. Hapalindoles: new alkaloids from the blue-green alga *Hapalosiphon fontinalis*. J. Am. Chem. Soc. 106(21):6456–57
49. Hillwig ML, Fuhrman HA, Ittiamornkul K, Sevco TJ, Kwak DH, Liu X. 2014. Identification and characterization of a welwitindolinone alkaloid biosynthetic gene cluster in the stigonematalean cyanobacterium *Hapalosiphon welwitschii*. ChemBioChem 15(5):665–69 [PubMed: 24677572]
50. Li S, Lowell AN, Yu F, Raveh A, Newmister SA, Bair N, et al. 2015. Hapalindole/ambiguine biogenesis is mediated by a cope rearrangement, C-C bond-forming cascade. J. Am. Chem. Soc. 137(49):15366–69 [PubMed: 26629885]
51. Chen T-Y, Chen J, Tang Y, Zhou J, Guo Y, Chang W. 2020. Pathway from N-alkylglycine to alkylisonitrile catalyzed by iron(II) and 2-oxoglutarate-dependent oxygenases. Angew. Chem. Int. Ed. 132(19):7437–41
52. Jonnalagadda R, Del Rio Flores A, Cai W, Mehmood R, Narayanamoorthy M, et al. 2021. Biochemical and crystallographic investigations into isonitrile formation by a non-heme iron-dependent oxidase/decarboxylase. J. Biol. Chem. 296:100231 [PubMed: 33361191]
53. Li H, Liu Y. 2020. Mechanistic investigation of isonitrile formation catalyzed by the nonheme iron/α-KG-dependent decarboxylase (ScoE). ACS Catal. 10(5):2942–57
54. Ali HS, Ghafoor S, De Visser SP. 2022. Density functional theory study into the reaction mechanism of isonitrile biosynthesis by the nonheme iron enzyme ScoE. Top. Catal. 65:528–43
55. La Pierre HS, Arnold J, Bergman RG, Toste FD. 2012. Carbon monoxide, isocyanide, and nitrile complexes of cationic, d^0 vanadium bisimides: π-back bonding derived from the π symmetry, bonding metal bisimido ligand orbitals. Inorg. Chem. 51(24):13334–44 [PubMed: 23181489]
56. Ugi I, Werner B, Domling A. 2003. The chemistry of isocyanides, their multicomponent reactions and their libraries. Molecules 8:53–66
57. Zhi S, Ma X, Zhang W. 2019. Consecutive multicomponent reactions for the synthesis of complex molecules. Org. Biomol. Chem. 17:7632–50 [PubMed: 31339143]
58. Wang Q, Wang D-X, Wang M-X, Zhu J. 2018. Still unconquered: enantioselective Passerini and Ugi multicomponent reactions. Acc. Chem. Res. 51:1290–300 [PubMed: 29708723]
59. Schäfer RJB, Monaco MR, Li M, Tirla A, Rivera-Fuentes P, Wennemers H. 2019. The bioorthogonal isonitrile–chlorooxime ligation. J. Am. Chem. Soc. 141:18644–48 [PubMed: 31710811]

60. Stöckmann H, Neves AA, Stairs S, Brindle KM, Leeper FJ. 2011. Exploring isonitrile-based click chemistry for ligation with biomolecules. Org. Biomol. Chem. 9:7303–5 [PubMed: 21915395]
61. Deb T, Franzini RM. 2020. The unique bioorthogonal chemistry of isonitriles. Synlett 31(10):938–44
62. Imming P, Mohr R, Müller E, Overheu W, Seitz G. 1982. [4 + 1]Cycloaddition of isocyanides to 1,2,4,5-tetrazines: a novel synthesis of pyrazole. Angew. Chem. 21(4):284
63. Tu J, Svatunek D, Parvez S, Liu AC, Levandowski BJ, et al. 2019. Stable, reactive, and orthogonal tetrazines: dispersion forces promote the cycloaddition with isonitriles. Angew. Chem. 58(27):9043–48 [PubMed: 31062496]
64. Wu H, Devaraj NK. 2018. Advances in tetrazine bioorthogonal chemistry driven by the synthesis of novel tetrazines and dienophiles. Acc. Chem. Res. 51(5):1249–59 [PubMed: 29638113]
65. Devaraj NK, Hilderbrand S, Upadhyay R, Mazitschek R, Weissleder R. 2010. Bioorthogonal turn-on probes for imaging small molecules inside living cells. Angew. Chem. 122(16):2931–34
66. Xu M, Tu J, Franzini RM. 2017. Rapid and efficient tetrazine-induced drug release from highly stable benzonorbornadiene derivatives. Chem. Commun. 53(46):6271–74
67. Xu M, Galindo-Murillo R, Cheatham TE, Franzini RM. 2017. Dissociative reactions of benzonorbornadienes with tetrazines: scope of leaving groups and mechanistic insights. Org. Biomol. Chem. 15(46):9855–65 [PubMed: 29139516]
68. Tu J, Xu M, Parvez S, Peterson RT, Franzini RM. 2018. Bioorthogonal removal of 3-isocyanopropyl groups enables the controlled release of fluorophores and drugs in vivo. J. Am. Chem. Soc. 140(27):8410–14 [PubMed: 29927585]
69. Tu J, Svatunek D, Parvez S, Eckvahl HJ, Xu M, Peterson RT, et al. 2020. Isonitrile-responsive and bioorthogonally removable tetrazine protecting groups. Chem. Sci. 11:169–79 [PubMed: 32110368]
70. Huang YB, Cai W, Del Rio Flores A, Twigg FF, Zhang W. 2020. Facile discovery and quantification of isonitrile natural products via tetrazine-based click reactions. Anal. Chem. 92(1):599–602 [PubMed: 31815449]
71. Stairs S, Neves AA, Stöckmann H, Wainman YA. 2013. Metabolic glycan imaging by isonitrile-tetrazine click chemistry. ChemBioChem 14:1063–67 [PubMed: 23670994]
72. Wainman YA, Neves AA, Stairs S, Stöckmann H, Ireland-Zecchini H, et al. 2013. Dual-sugar imaging using isonitrile and azido-based click chemistries. Org. Biomol. Chem. 11(42):7297–300 [PubMed: 24065211]
73. Tørring T, Shames SR, Cho W, Roy CR, Crawford JM. 2017. Acyl histidines: new *N*-acyl amides from *Legionella pneumophila*. ChemBioChem 18(7):638–46 [PubMed: 28116768]
74. Richards JP, Cai W, Zill NA, Zhang W, Ojha AK. 2019. Adaptation of *Mycobacterium tuberculosis* to biofilm growth is genetically linked to drug tolerance. Antimicrob. Agents Chemother. 63(11):e01213–19 [PubMed: 31501144]
75. Del Rio Flores A, Twigg FF, Du Y, Cai W, Aguirre DQ, et al. 2021. Biosynthesis of triacsin featuring an *N*-hydroxytriazene pharmacophore. Nat. Chem. Biol. 17:1305–13 [PubMed: 34725510]
76. Twigg FF, Cai W, Huang W, Liu J, Sato M, Perez TJ, et al. 2019. Identifying the biosynthetic gene cluster for triacsins with an *N*-hydroxytriazene moiety. ChemBioChem 20(9):1145–49 [PubMed: 30589194]
77. Kino T, Hatanaka H, Miyata S, Inamura N, Kohsaka M, Aoki H, et al. 1987. FK-506, a novel immunosuppressant isolated from a *Streptomyces*. J. Antibiot. 40:1256–65
78. Ittiamornkul K, Zhu Q, Gkotsi DS, Smith DRM, Hillwig ML, Nightingale N, et al. 2015. Promiscuous indolyl vinyl isonitrile synthases in the biogenesis and diversification of hapalindole-type alkaloids. Chem. Sci. 6(12):6836–40 [PubMed: 29861925]
79. Bunn BM, Xu M, Webb CM, Viswanathan R. 2021. Biocatalysts from cyanobacterial hapalindole pathway afford antivirulent isonitriles against MRSA. J. Biosci. 46:37 [PubMed: 33952728]
80. Liu Z, Ioerger TR, Wang F, Sacchettini JC. 2013. Structures of *Mycobacterium tuberculosis* FadD10 protein reveal a new type of adenylate-forming enzyme. J. Biol. Chem. 288(25):18473–83 [PubMed: 23625916]

81. Chhabra A, Haque AS, Pal RK, Goyal A, Rai R, Joshi S, et al. 2012. Nonprocessive [2 + 2]e^- off-loading reductase domains from mycobacterial nonribosomal peptide synthetases. PNAS 109(15):5681–86 [PubMed: 22451903]
82. Lee M, Lenman M, Banaś A, Bafor M, Singh S, Lee M, et al. 1998. Identification of non-heme diiron proteins that catalyze triple bond and epoxy group formation. Science 280(5365):915–18 [PubMed: 9572738]
83. Chai Q-Y, Yang Z, Lin H-W, Han B-N. 2016. Alkynyl-containing peptides of marine origin: a review. Mar. Drugs 14(11):216 [PubMed: 27886049]
84. Zhu X, Liu J, Zhang W. 2015. *De novo* biosynthesis of terminal alkyne-labeled natural products. Nat. Chem. Biol. 11(2):115–20 [PubMed: 25531891]
85. Marchand JA, Neugebauer ME, Ing MC, Lin CI, Pelton JG, Chang MCY. 2019. Discovery of a pathway for terminal-alkyne amino acid biosynthesis. Nature. 567(7748):420–24 [PubMed: 30867596]
86. Scinto SL, Bilodeau DA, Hincapie R, Lee W, Nguyen SS, et al. 2021. Bioorthogonal chemistry. Nat. Rev. Methods Prim. 1:29
87. Dieterich DC, Link AJ, Graumann J, Tirrell DA, Schuman EM. 2006. Selective identification of newly synthesized proteins in mammalian cells using bioorthogonal noncanonical amino acid tagging (BONCAT). PNAS 103(25):9482–87 [PubMed: 16769897]
88. Zhu X, Zhang W. 2015. Tagging polyketides/non-ribosomal peptides with a clickable functionality and applications. Front. Chem. 3:11 [PubMed: 25815285]
89. Bai Y, McCoy JG, Levin EJ, Sobrado P, Rajashankar KR, et al. 2015. X-ray structure of a mammalian stearoyl-CoA desaturase. Nature 524(7564):252–56 [PubMed: 26098370]
90. Shen J, Wu G, Tsai AL, Zhou M. 2020. Structure and mechanism of a unique diiron center in mammalian stearoyl-CoA desaturase. J. Mol. Biol. 432(18):5152–61 [PubMed: 32470559]
91. Zhu X, Su M, Manickam K, Zhang W. 2015. Bacterial genome mining of enzymatic tools for alkyne biosynthesis. ACS Chem. Biol. 10(12):2785–93 [PubMed: 26441143]
92. Potgieter HC, Vermeulen NMJ, Potgieter DJJ, Strauss HF. 1977. A toxic amino acid, 2(S)3(R)-2-amino-3-hydroxypent-4-ynoic acid from the fungus *Sclerotium rolfsii*. Phytochemistry 16(11):1757–59
93. Sanada M, Miyano T, Iwadare S. 1986. β-Ethynylserine, an antimetabolite of L-threonine, from *Streptomyces cattleya*. J. Antibiot. 39(2):304–5
94. Scannell JP, Pruess DL, Demny TG, Weiss F, Williams T, Stempel A. 1971. Antimetabolites produced by microorganisms. II. L-2-amino-4-pentynoic acid. J. Antibiot. 24(4):239–44
95. Sanada M, Tetsuji M, Iwadare S. 1986. Biosynthesis of fluorothreonine and fluoroacetic acid by the thienamycin producer, *Streptomyces cattleya*. J. Antibiot. 39:259–64
96. Neugebauer ME, Sumida KH, Pelton JG, McMurry JL, Marchand JA, Chang MCY. 2019. A family of radical halogenases for the engineering of amino-acid-based products. Nat. Chem. Biol. 15(10):1009–16 [PubMed: 31548692]
97. Prescher JA, Bertozzi CR. 2005. Chemistry in living systems. Nat. Chem. Biol. 1:13–21 [PubMed: 16407987]
98. Grammel M, Hang HC. 2013. Chemical reporters for biological discovery. Nat. Chem. Biol. 9(8):475–84 [PubMed: 23868317]
99. Kolb HC, Finn MG, Sharpless KB. 2001. Click chemistry: diverse chemical function from a few good reactions. Angew. Chem. 40(11):2004–21 [PubMed: 11433435]
100. Zhu X, Shieh P, Su M, Bertozzi CR, Zhang W. 2016. A fluorogenic screening platform enables directed evolution of an alkyne biosynthetic tool. Chem. Commun. 52(75):11239–42
101. Moss NA, Seiler G, Leão TF, Castro-Falcón G, Gerwick L, et al. 2019. Nature's combinatorial biosynthesis produces vatiamides A–F. Angew. Chem. 131(27):9125–29
102. Murata K, Suenaga M, Kai K. 2021. Genome mining discovery of protegenins A–D, bacterial polyynes involved in the antioomycete and biocontrol activities of Pseudomonas protegens. ACS Chem. Biol. In press

103. Kai K, Sogame M, Sakurai F, Nasu N, Fujita M. 2018. Collimonins A-D, unstable polyynes with antifungal or pigmentation activities from the fungus-feeding bacterium *Collimonas fungivorans* Ter331. Org. Lett. 20(12):3536–40 [PubMed: 29792438]
104. Ross C, Scherlach K, Kloss F, Hertweck C. 2014. The molecular basis of conjugated polyyne biosynthesis in phytopathogenic bacteria. Angew. Chem. 53(30):7794–98 [PubMed: 24898429]
105. Zhang J, Liang L, Guan X, Deng R, Qu H, et al. 2018. In situ, accurate, surface-enhanced Raman scattering detection of cancer cell nucleus with synchronous location by an alkyne-labeled biomolecular probe. Anal. Bioanal. Chem. 410(2):585–94 [PubMed: 29214531]
106. Jamieson LE, Greaves J, McLellan JA, Munro KR, Tomkinson NCO, et al. 2018. Tracking intracellular uptake and localisation of alkyne tagged fatty acids using Raman spectroscopy. Spectrochim. Acta A 197:30–36
107. Yamaguchi S, Matsushita T, Izuta S, Katada S, Ura M, Ikeda T, et al. 2017. Chemically-activatable alkyne-tagged probe for imaging microdomains in lipid bilayer membranes. Sci. Rep. 7:41007 [PubMed: 28117375]
108. Seidel J, Miao Y, Porterfield W, Cai W, Zhu X, et al. 2019. Structure-activity-distribution relationship study of anti-cancer antimycin-type depsipeptides. Chem. Commun. 55:9379–82
109. Moliner F, Knox K, Gordon D, Lee M, Tipping WJ, Geddis A, et al. 2021. A palette of minimally tagged sucrose analogues for real-time Raman imaging of intracellular plant metabolism. Angew. Chem. 133(14):7715–20
110. Hu F, Chen Z, Zhang L, Shen Y, Wei L, Min W. 2015. Vibrational imaging of glucose uptake activity in live cells and tissues by stimulated Raman scattering. Angew. Chem. 54(34):9821–25 [PubMed: 26207979]
111. Yan Y, Chen J, Zhang L, Zheng Q, Han Y, Zhang H, et al. 2013. Multiplexing of combinatorial chemistry in antimycin biosynthesis: expansion of molecular diversity and utility. Angew Chem. 125(47):12534–38
112. Sandy M, Rui Z, Gallagher J, Zhang W. 2012. Enzymatic synthesis of dilactone scaffold of antimycins. ACS Chem. Biol. 7(12):1956–61 [PubMed: 22971101]
113. Hatzenpichler R, Krukenberg V, Spietz RL, Jay ZJ. 2020. Next-generation physiology approaches to study microbiome function at single cell level. Nat. Rev. Microbiol. 18(4):241–56 [PubMed: 32055027]
114. Johnson JA, Lu YY, Van Deventer JA, Tirrell DA. 2010. Residue-specific incorporation of non-canonical amino acids into proteins: recent developments and applications. Curr. Opin. Chem. Biol. 14(6):774–80 [PubMed: 21071259]
115. Horwich AL, Farr GW, Fenton WA. 2006. GroEL–GroES-mediated protein folding. Chem. Rev. 106(5):1917–30 [PubMed: 16683761]
116. Truong F, Yoo TH, Lampo TJ, Tirrell DA. 2012. Two-strain, cell-selective protein labeling in mixed bacterial cultures. J. Am. Chem. Soc. 134(20):8551–56 [PubMed: 22575034]
117. Morita H, Yamashita M, Shi SP, Wakimoto T, Kondo S, et al. 2011. Synthesis of unnatural alkaloid scaffolds by exploiting plant polyketide synthase. PNAS 108(33):13504–9 [PubMed: 21825160]
118. Williams GJ. 2013. Engineering polyketide synthases and nonribosomal peptide synthetases. Curr. Opin. Struct. Biol. 23(4):603–12 [PubMed: 23838175]
119. Su M, Zhu X, Zhang W. 2018. Probing the acyl carrier protein-enzyme interactions within terminal alkyne biosynthetic machinery. AIChE J. 64(12):4255–62 [PubMed: 30983594]
120. Porterfield WB, Poenateetai N, Zhang W. 2020. Engineered biosynthesis of alkyne-tagged polyketides by type I PKSs. iScience 23(3):100938 [PubMed: 32146323]
121. Bihlmaier C, Welle E, Hofmann C, Welzel K, Vente A, et al. 2006. Biosynthetic gene cluster for the polyenoyltetramic acid α-lipomycin. Antimicrob. Agents Chemother. 50(6):2113–21 [PubMed: 16723573]
122. Whicher JR, Smaga SS, Hansen DA, Brown WC, Gerwick WH, et al. 2013. Cyanobacterial polyketide synthase docking domains: a tool for engineering natural product biosynthesis. Chem. Biol. 20(11):1340–51 [PubMed: 24183970]

123. Fischbach MA, Walsh CT. 2006. Assembly-line enzymology for polyketide and nonribosomal peptide antibiotics: logic machinery, and mechanisms. Chem. Rev. 106(8):3468–96 [PubMed: 16895337]

124. Liu J, Zhu X, Kim SJ, Zhang W. 2016. Antimycin-type depsipeptides: discovery, biosynthesis, chemical synthesis, and bioactivities. Nat. Prod. Rep. 33(10):1146–65 [PubMed: 27307039]

125. Awakawa T, Fujioka T, Zhang L, Hoshino S, Hu Z, et al. 2018. Reprogramming of the antimycin NRPSPKS assembly lines inspired by gene evolution. Nat. Commun. 9:3534 [PubMed: 30166552]

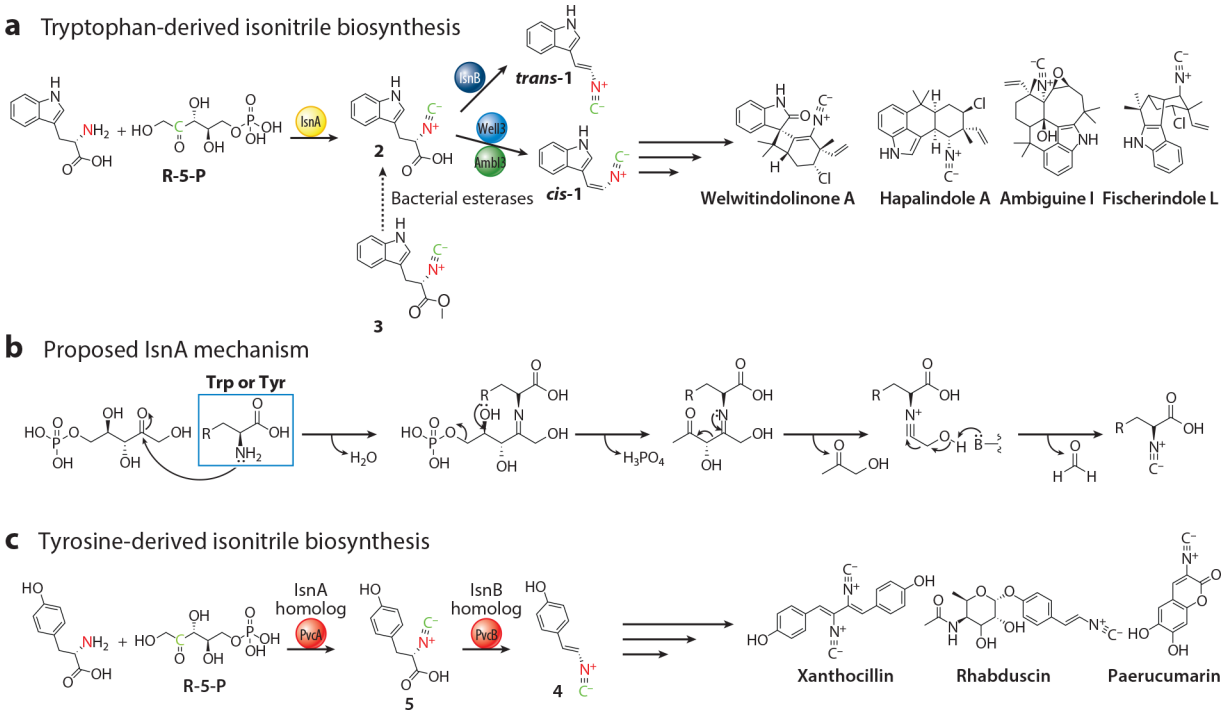

Figure 1.

Isonitrile biosynthesis by IsnA synthases. (*a*) IsnA, an isonitrile synthase, catalyzes the condensation reaction between the α-amino group of L-tryptophan and C2 of ribulose-5-phosphate (R-5-P) to form the isonitrile group. IsnB, a Fe(II)/α-KG-dioxygenase, promotes oxidative decarboxylation to generate *trans*-**1**. Well3 and AmbI3, homologs of IsnB, catalyze a similar reaction that affords *cis*-**1**. (*b*) The proposed mechanism for IsnA synthases. (*c*) PvcA and PvcB promote analogous reactions to IsnA and IsnB, except L-tyrosine is used. Figure adapted with permission from Zhang et al. (8); copyright 2020 John Wiley and Sons; Brady & Clardy (29, 36); copyright 2005 John Wiley and Sons; and Chang et al. (37); copyright 2017 American Chemical Society.

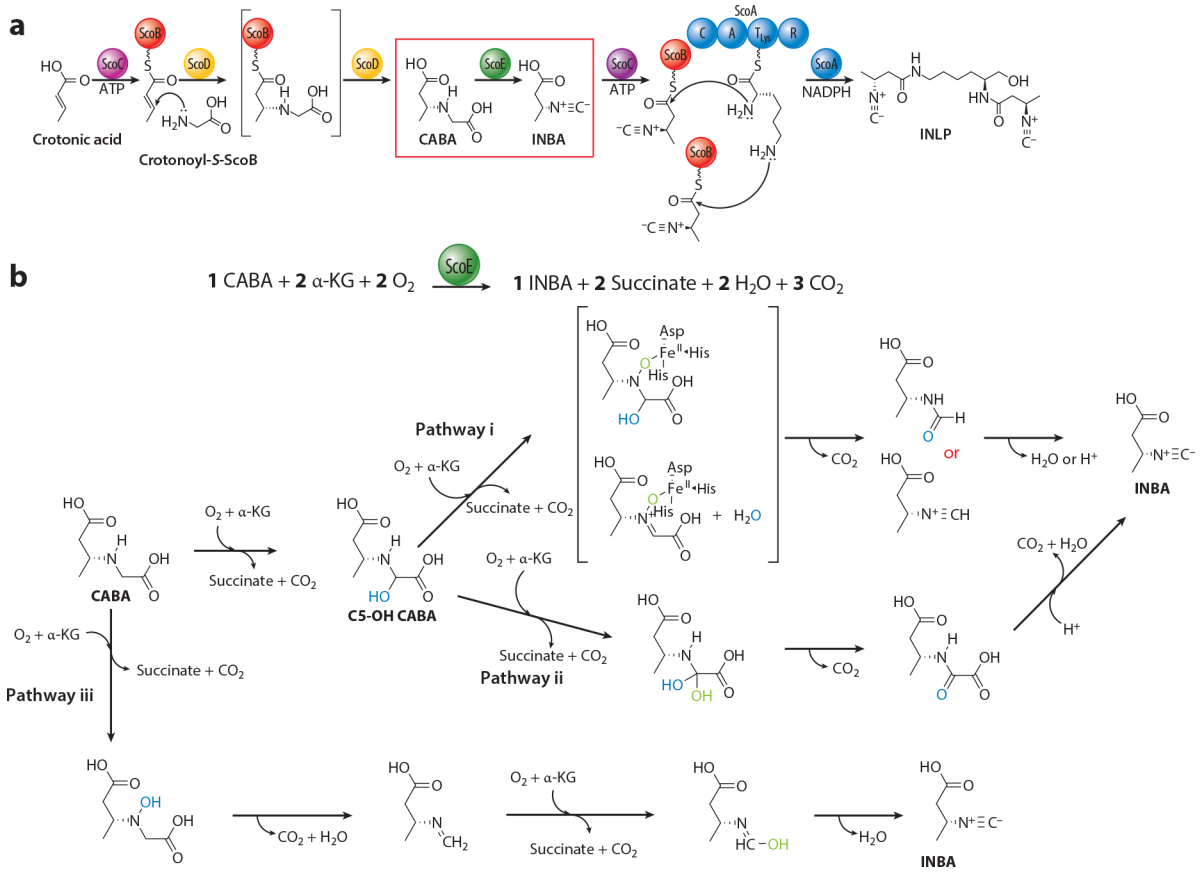

Figure 2.

Isonitrile biosynthesis by Fe(II)/α-KG-dioxygenases. (*a*) The INLP biosynthetic pathway from *Streptomyces coeruleorubidus* with an emphasis on ScoE, a Fe(II)/α-KG-dioxygenase, that catalyzes oxidative decarboxylation of CABA to afford INBA. (*b*) There are three proposed mechanisms for isonitrile formation by ScoE differing at the site(s) of hydroxylation. Two α-KG half reactions are required, as shown in the scheme. Abbreviations: A, adenylation; C, condensation; CABA, (R)-3-[(carboxymethyl)amino]butanoic acid; INBA, (R)-3-isocyanobutanoic acid; INLP, isonitrile lipopeptide; T, thiolation. Figure adapted with permission from Harris et al. (30); copyright 2018 John Wiley and Sons and Jonnalagadda et al. (52); copyright 2021 Elsevier.

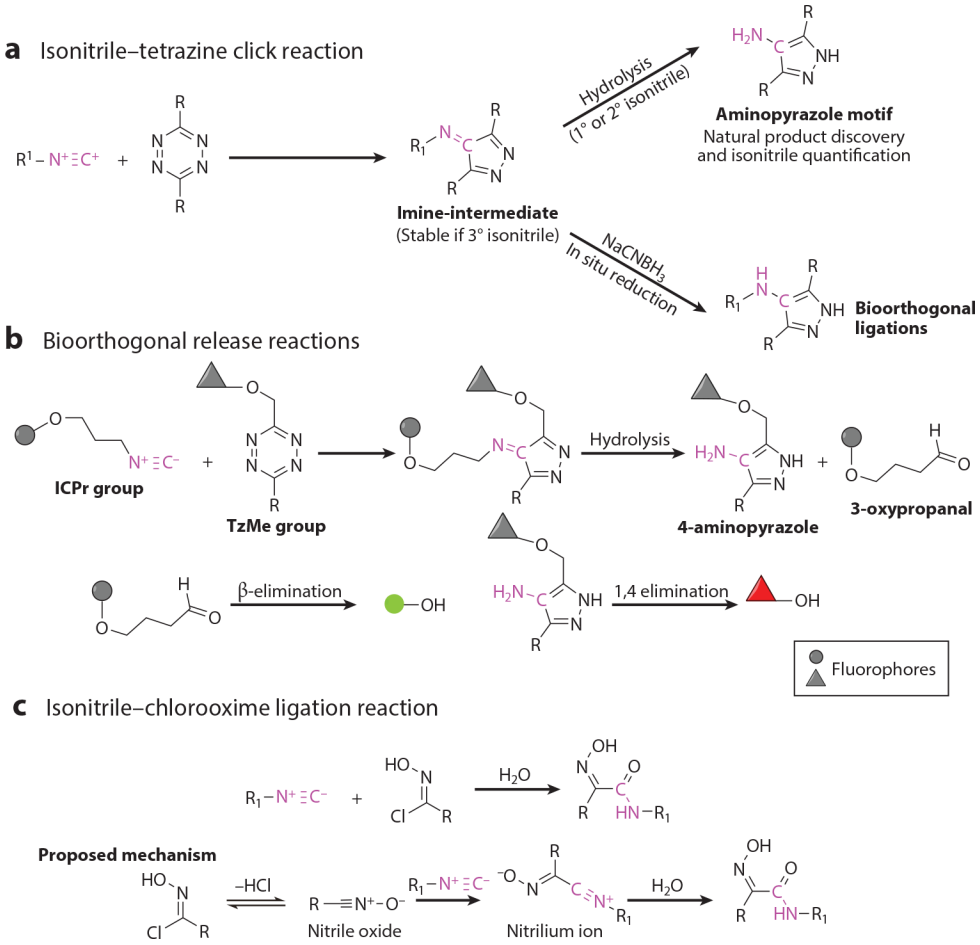

Figure 3.

Bioorthogonal chemistry of isonitriles. (*a*) Click reaction between isonitrile and tetrazine. An in situ reduction of the imine intermediate with $NaCNBH_3$ yields a conjugate that can be applied to bioorthogonal ligations. (*b*) Bioorthogonal release chemistry using ICPr and TzMe groups that release two fluorophores after spontaneous hydrolysis of the imine intermediate and elimination reactions. (*c*) The isonitrile–chlorooxime bioorthogonal reaction yielding a hydroxyimino amide product. Figure adapted with permission from Schäfer et al. (59); copyright 2019 American Chemical Society; Tu et al. (69) (CC BY-SA 3.0); and Huang et al. (70); copyright 2020 American Chemical Society.

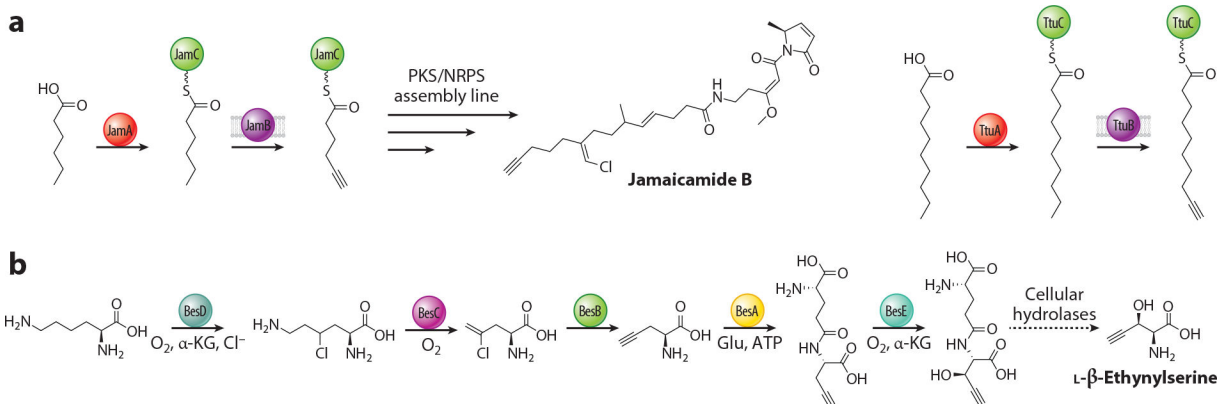

Figure 4.

Terminal-alkyne biosynthetic pathways. (*a*) The JamABC system uses the membrane-bound bifunctional desaturase/acetylenase JamB to generate 5-hexynoyl-*S*-JamC. The TtuABC system works analogously with a C10 fatty acid preference. (*b*) The biosynthetic pathway of L-β-ethynylserine consisting of BesB, a PLP-dependent enzyme that catalyzes γ-elimination of chloride to form the terminal alkyne. Abbreviations: NRPS, nonribosomal peptide synthetase; PKS, polyketide synthase. Figure adapted with permission from Zhu et al. (84); copyright 2015 Nature Publishing Group, and Marchand et al. (85); copyright 2019 Nature Publishing Group.

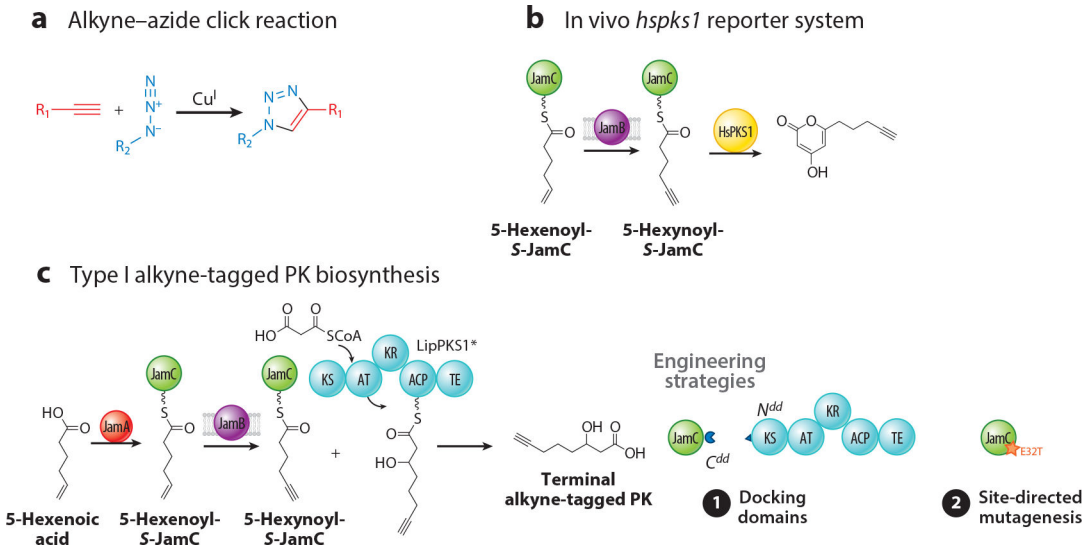

Figure 5.

Bioorthogonal chemistry and engineering of alkynyl molecules. (*a*) Cu(I)-catalyzed click reaction between azides and alkynes. (*b*) The in vivo *hspks1* reporter system encodes a type III PKS with unusually broad substrate tolerance that generates a pyrone scaffold when supplied with a hexynoyl moiety. (*c*) Overview of biosynthetic scheme to generate alkyne-tagged polyketides. Docking domain and site-directed mutagenesis were used to improve ACP-KS interactions. Abbreviations: ACP, acyl carrier protein; AT, acyltransferase; KR, ketoreductase; KS, ketosynthase; PKS, polyketide synthase; TE, thioesterase. Figure adapted with permission from Zhu et al. (84); copyright 2015 Nature Publishing Group and Porterfield et al. (120); copyright 2020 Elsevier.